

SAGAS: Semantic-Aware Graph-Assisted Stitching for Offline Temporal Logic Planning[★]

Ruijia Liu^{*} Ancheng Hou^{*} Shaoyuan Li^{*} Xiang Yin^{*}

^{*} School of Automation and Intelligent Sensing, Shanghai Jiao Tong University,
Shanghai 200240, China (e-mail: {liuruijia, hou.ancheng, syli, yinxiang}@
sjtu.edu.cn).

Abstract: Linear Temporal Logic (LTL) provides a rigorous framework for complex robotic tasks, yet existing methods often rely on accurate dynamics models or expensive online interactions. In this work, we address LTL-constrained control in a challenging offline, model-free setting, utilizing only fixed, task-agnostic datasets of fragmented trajectories. We propose **SAGAS**, a novel framework combining graph-assisted trajectory stitching with automata-guided planning. First, we construct a latent reachability graph from a learned temporal-distance representation. To bridge the semantic gap, we augment this graph with certified anchor nodes and probabilistic soft labels. We then translate the specification into a Büchi automaton and search the implicit product space to derive a cost-minimal prefix-suffix plan. Finally, a subgoal-conditioned low-level policy is deployed to execute these latent waypoints. Experiments on OGBench locomotion domains demonstrate that SAGAS successfully synthesizes efficient trajectories for diverse LTL tasks, effectively bridging the gap between fragmented offline data and complex logical constraints.

Keywords: Linear Temporal Logic, Hierarchical Planning, Offline Reinforcement Learning

1. INTRODUCTION

Formal specifications such as Linear Temporal Logic (LTL), provide a rigorous framework for encoding complex robotic tasks beyond simple point-to-point navigation, such as persistent surveillance and sequential assembly Kloetzer and Belta (2008); Baier and Katoen (2008); Scher and Kress-Gazit (2020). While classical model-based approaches effectively handle these constraints via product automata search Fainekos et al. (2005); Smith et al. (2011); Ren et al. (2024), they depend on accurate system dynamics, which are often unavailable in real-world scenarios. Model-free Reinforcement Learning (RL) offers an alternative by embedding logical objectives into rewards Hasanbeig et al. (2018); Voloshin et al. (2023); Shah et al. (2024) or decomposing tasks into subgoals Qiu et al. (2023); Jackermeier and Abate (2025); Guo et al. (2025). However, these methods typically require extensive online interaction for each new specification and struggle to generalize to unseen temporal patterns or subgoals.

In contrast, *offline* RL aims to synthesize behaviors solely from fixed, task-agnostic datasets without environment interaction. Recent advances in Graph-Assisted Stitching (GAS) Baek et al. (2025); Opryshko et al. (2025) have demonstrated that long-horizon reachability can be recovered from fragmented trajectories by constructing a latent graph based on temporal-distance learning. Yet, existing GAS methods are inherently designed for single-goal navigation; they lack the *semantic awareness* required to reason about the multi-stage, cyclic, and safety-critical constraints imposed by LTL. Bridging this gap requires a mechanism that can interpret task-agnostic geometric data through the lens of task-specific logical symbols.

[★] This work was supported by the National Natural Science Foundation of China (62573291, 62173226).

Project page: <https://cps-sjtu.github.io/SAGAS>

In this work, we propose **SAGAS**, a framework that extends trajectory stitching to arbitrary LTL tasks in a fully offline, model-free setting. To bridge the gap between fragmented, task-agnostic datasets and complex logical requirements, our method first extends the GAS latent graph construction by introducing a semantic augmentation mechanism, enriching the geometric topology with probabilistic soft labels and certified anchor nodes. Building on this, we perform search over the implicit product of the augmented latent graph and a Büchi automaton to synthesize cost-efficient prefix-suffix plans, which subsequently guide a learned low-level policy to execute the task. Evaluations on the OGBench Park et al. (2025) locomotion domains demonstrate that SAGAS scales robustly to giant-scale environments and complex constraints, effectively stitching disjoint behaviors. Furthermore, comparative analyses confirm that our joint optimization in the product space significantly reduces physical execution steps compared to decoupled planning baselines.

2. RELATED WORKS

2.1 Reinforcement Learning for Temporal Logic Tasks

Standard RL approaches for LTL typically rely on reward shaping or automata-based reward machines to guide exploration Hasanbeig et al. (2018); Bagatella et al. (2024); Voloshin et al. (2023); Shah et al. (2024). To facilitate task generalization, hierarchical methods decompose LTL formulas into sequences of subgoals handled by modular skills Qiu et al. (2023); Liu et al. (2024); Jackermeier and Abate (2025); Guo et al. (2025). These approaches allow learned primitives to be reused across different specifications, thereby reducing the sample complexity for new tasks. However, these predominantly online approaches require expensive interaction to learn these task-specific policies. Furthermore, their generalization capability is often contingent

upon a *pre-defined* library of skills or subgoals, limiting their adaptability to tasks involving novel or unseen subgoals. Our method, by contrast, operates strictly offline and leverages graph search to flexibly compose behaviors for arbitrary specifications without relying on a fixed set of pre-defined skills.

2.2 Offline RL and Graph-Based Stitching

Offline Goal-Conditioned RL (GCRL) exploits structural information in static datasets to learn multi-task policies Andrychowicz et al. (2017); Kostrikov et al. (2022); Park et al. (2023). To address the “horizon gap” in fragmented datasets, Graph-Assisted Stitching (GAS) methods Baek et al. (2025); Opryshko et al. (2025) employ a *hierarchical* planning scheme. They explicitly construct reachability graphs in latent or state spaces to perform high-level search, which then guides a low-level policy to stitch local trajectories into global paths. While highly effective for goal-reaching, these geometric planners are oblivious to semantic constraints and temporal logic. We extend this hierarchical paradigm by integrating semantic augmentation and automata-theoretic planning, thereby elevating trajectory stitching from simple goal-reaching to complex logical satisfaction.

2.3 Generative Planning for LTL

Recent works have explored generative models for LTL planning. For instance, the framework of Doppler was proposed in Feng et al. (2025) by integrating diffusion models into a hierarchical RL framework, training a high-level policy to select options based on LTL progression. While effective for tasks amenable to receding-horizon planning (e.g., co-safe LTL), it relies on a learned high-level policy and local lookahead. This design lacks the explicit structural guarantees required for infinite-horizon cyclic behaviors and necessitates training a new high-level policy for complex logical dependencies. In contrast, our method avoids high-level policy learning entirely. By performing explicit graph search over the product of a latent graph and a Büchi automaton, we naturally handle general LTL specifications, which may require infinite-horizon recurrence, while ensuring efficiency through graph-based cost minimization.

3. PRELIMINARIES

3.1 System Model

We consider a discrete-time dynamical system with unknown transition dynamics, defined over a continuous state space $\mathcal{S} \subseteq \mathbb{R}^{d_s}$ and an action space $\mathcal{A} \subseteq \mathbb{R}^{d_a}$. The system evolution is governed by

$$s_{t+1} = f(s_t, a_t), \quad (1)$$

where $f : \mathcal{S} \times \mathcal{A} \rightarrow \mathcal{S}$ is an *unknown* deterministic transition function. To relate the system state to high-level tasks, we define a projection map $\Pi : \mathcal{S} \rightarrow \mathcal{X}$, where $\mathcal{X} \subseteq \mathbb{R}^{d_t}$ denotes the *task space* (e.g., robot workspace or end-effector position). While the control inputs act on the high-dimensional state space \mathcal{S} , the logical predicates defining the task objectives are specified over the lower-dimensional task space \mathcal{X} .

3.2 Linear Temporal Logic Task

Atomic Propositions. Let $\mathcal{AP} = \{\ell_1, \dots, \ell_m\}$ denote a finite set of atomic propositions. Each proposition $\ell \in \mathcal{AP}$ corresponds to a specific labeled region $\mathcal{R}_\ell \subseteq \mathcal{X}$ in the task

space. Following standard practice in LTL planning Vasile and Belta (2013), we assume these regions are pairwise disjoint. We define a labeling function $L : \mathcal{S} \rightarrow 2^{\mathcal{AP}}$ as $L(s) = \{\ell \in \mathcal{AP} \mid \Pi(s) \in \mathcal{R}_\ell\}$, which maps each state s to the set of atomic propositions satisfied at its projection $\Pi(s)$.

Linear Temporal Logic. We specify high-level tasks using Linear Temporal Logic without the “next” operator ($\text{LTL}_{\neg X}$), which is widely adopted for specifying navigation-style robotic tasks in continuous space Kloetzer and Belta (2008). The syntax of $\text{LTL}_{\neg X}$ is recursively defined as:

$$\phi ::= \text{true} \mid \ell \in \mathcal{AP} \mid \neg\phi \mid \phi_1 \wedge \phi_2 \mid \phi_1 \text{ U } \phi_2,$$

where \neg and \wedge denote logical negation and conjunction, respectively, and U is the “until” operator. Common temporal operators such as “eventually” ($\text{F}\phi = \text{true U } \phi$) and “always” ($\text{G}\phi = \neg\text{F}\neg\phi$) are derived as standard abbreviations. Given a trajectory $\tau = s_0 s_1 s_2 \dots$, the sequence of labels $L(s_0)L(s_1)L(s_2)\dots$ constitutes an infinite word $\sigma \in (2^{\mathcal{AP}})^\omega$. We write $\tau \models \phi$ if the induced word σ satisfies ϕ according to standard LTL semantics Baier and Katoen (2008). Any LTL formula ϕ can be translated into a Nondeterministic Büchi Automaton (NBA) $\mathcal{B} = (Q, Q_0, \Sigma, \delta, F)$, where $\Sigma = 2^{\mathcal{AP}}$ is the alphabet. An infinite run $\rho = q_0 q_1 \dots$ is accepting if it visits the set of accepting states F infinitely often. Consequently, any accepting run can be decomposed into a finite *prefix* reaching a state $q_f \in F$, followed by a *suffix* cycle starting and ending at q_f .

3.3 Problem Setting

We consider an *offline* setting where the agent has no knowledge of the system model (1) and cannot interact with the environment during training. Instead, learning relies solely on a static dataset

$$\mathcal{D} = \{\tau^{(i)}\}_{i=1}^N, \quad \tau^{(i)} = (s_0^{(i)}, a_0^{(i)}, s_1^{(i)}, a_1^{(i)}, \dots),$$

comprising trajectories of varying lengths collected by unknown behavior policies. Crucially, these trajectories are task-agnostic and fragmented; they typically represent short-term behaviors and do *not* individually demonstrate the long-horizon requirements of the target specification. No additional online data collection is permitted.

Given an initial state s_0 and an arbitrary $\text{LTL}_{\neg X}$ specification ϕ , the objective is to synthesize a control policy that generates a trajectory τ satisfying $\tau \models \phi$. Beyond logical satisfaction, we seek to minimize execution cost. Leveraging the prefix-suffix structure of Büchi acceptance, we define the efficiency metric as:

$$J(\tau) = \lambda T_{\text{pre}}(\tau) + (1 - \lambda) T_{\text{suf}}(\tau), \quad (2)$$

where $T_{\text{pre}}(\tau)$ denotes the time steps required to complete the prefix, $T_{\text{suf}}(\tau)$ denotes the period of the suffix cycle, and $\lambda \in [0, 1]$ is a user-defined weight balancing transient and steady-state performance. Our goal is to find a policy that ensures $\tau \models \phi$ while minimizing $J(\tau)$.

Remark 1. It is important to clarify the definition of “policy” in this framework. Rather than a monolithic end-to-end mapping, our solution will adopt a *hierarchical* structure consistent with offline hierarchical RL. The “synthesized policy” effectively consists of a task-specific high-level plan (a sequence of latent subgoals representing the prefix and suffix) and a reusable, task-agnostic low-level policy trained to reach these subgoals. This distinction is vital in the offline setting, as it allows the agent to stitch together diverse sub-optimal fragments from the dataset to realize complex, unseen tasks without retraining the low-level controller.

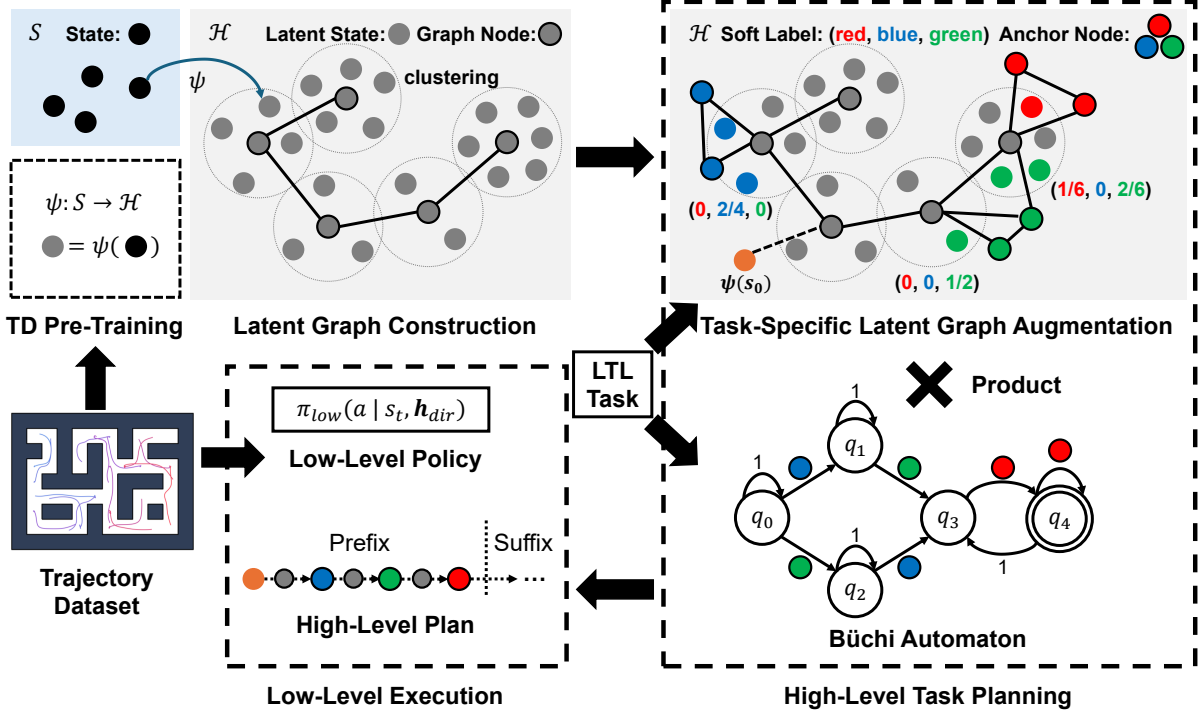


Fig. 1. Overview of the the proposed SAGAS framework.

4. OUR METHOD

In this section, we describe in detail the proposed method for offline temporal logic planning.

4.1 Overview

To bridge the gap between fragmented, task-agnostic offline data and the requirement for long-horizon logical satisfaction, we propose SAGAS (Semantic-Aware Graph-Assisted Stitching), a hierarchical framework capable of stitching local behavioral fragments into globally efficient behaviors. SAGAS builds upon the *Graph-Assisted Stitching* (GAS) Baek et al. (2025) framework, adopting its temporal-distance representation and clustering-based graph construction scheme. In this learned latent space, the Euclidean distance encodes the minimal step-to-go. We extend this geometric substrate to LTL tasks by endowing the latent graph with semantic structure and performing automata-guided search. Crucially, thanks to the alignment between latent geometry and temporal duration, optimizing path cost in the graph serves as a direct **proxy** for reducing the weighted execution cost $J(\tau)$ defined in (2).

As illustrated in Fig. 1, the proposed pipeline is structured into four distinct stages:

- (1) **Offline Representation Learning & Graph Construction:** Starting from the trajectory dataset, we perform **TD Pre-Training** to learn a temporal-distance representation ψ and simultaneously train a **Low-Level Policy** π_{low} . We then cluster the embedded states to perform **Latent Graph Construction**, creating a reusable topological substrate that captures long-horizon reachability independent of downstream tasks.
- (2) **Task-Specific Latent Graph Augmentation:** Given an LTL task, we bridge the geometric latent space with discrete logic by annotating the graph. This involves estimating *soft labels* for nodes based on probabilistic

estimation and inserting *anchor nodes* that serve as certified realizations of atomic propositions.

- (3) **High-Level Task Planning:** We translate the LTL specification into a Büchi automaton and search the implicit **product** of this automaton and the augmented latent graph. This search yields a **cost-minimal** high-level plan (with respect to the latent metric) comprising a prefix path and a suffix cycle.
- (4) **Low-Level Execution:** Finally, the agent executes the synthesized high-level plan using the pre-trained Low-Level Policy. The policy tracks the sequence of latent subgoals (prefix followed by the repeating suffix), thereby realizing the infinite-horizon behavior required by the specification.

By stitching fragmented offline data, our framework synthesizes logically correct and efficient plans, enabling zero-shot generalization to arbitrary tasks without explicit demonstrations.

4.2 Offline Latent Graph Construction

We utilize the Graph-Assisted Stitching (GAS) framework Baek et al. (2025) to abstract the raw offline dataset into a compact *latent graph*. This process is performed entirely offline and consists of two phases: learning a temporal-distance representation and constructing the topological graph. Unless stated otherwise, we adopt the implementation details and hyperparameters from GAS.

Temporal Distance (TD) Representation. First, we learn an embedding function $\psi : S \rightarrow H$ such that the Euclidean distance $\|\psi(s) - \psi(g)\|_2$ approximates the minimal dynamical step count (temporal distance) between states s and g . Following GAS, this is formulated as a goal-conditioned value estimation problem, where the value function is defined as the negative latent distance. We train this value proxy using Implicit Q-

Learning (IQL) Kostrikov et al. (2022) with expectile regression, ensuring the latent geometry aligns with system reachability.

TD-Aware Graph Construction. Using the learned embedding ψ , we construct a directed graph $\mathcal{H}_{\text{graph}} = (\mathcal{V}, \mathcal{E}, w)$ to capture feasible transitions. We employ the iterative clustering procedure from GAS to discretize the continuous latent space. Raw states are grouped into clusters such that cluster centers (the nodes \mathcal{V}) are spaced approximately H_{TD} temporal steps apart. Directed edges (u, v) are added if the latent distance satisfies $\|u - v\|_2 \leq H_{\text{TD}}$, weighted by $w(u, v) = \|u - v\|_2$. To enhance graph reliability, we apply the Temporal Efficiency (TE) metric Baek et al. (2025) to prune states associated with noisy or suboptimal transitions before clustering.

Modification for LTL Tasks: A critical deviation from the original GAS pipeline is our retention of the raw data mapping. While GAS operates purely in latent space after construction, we explicitly store the correspondence between each latent node v and its constituent raw states:

$$\text{node2raw}(v) = \{s \in \mathcal{S} \mid \psi(s) \in \mathcal{C}_v\}. \quad (3)$$

Preserving this set is essential for our method, as it enables the grounding of abstract latent nodes to task-space atomic propositions during the subsequent semantic augmentation phase.

4.3 Low-Level Policy Training

To execute plans generated on the latent graph, we train a goal-conditioned low-level policy $\pi_{\text{low}}(a \mid s_t, \mathbf{h}_{\text{dir}})$ using the offline dataset. Crucially, to ensure consistency between the planning and execution horizons, the policy is trained to reach subgoals located exactly H_{TD} steps into the future (matching the graph’s edge length). The goal is parameterized as a normalized direction vector in the latent space:

$$\mathbf{h}_{\text{dir}} = \frac{\psi(s_{t+H_{\text{TD}}}) - \psi(s_t)}{\|\psi(s_{t+H_{\text{TD}}}) - \psi(s_t)\|}.$$

This directional conditioning allows the policy to generalize across positions by focusing on relative traversal directions rather than absolute coordinates. The policy is optimized using the DDPG+BC objective Fujimoto and Gu (2021), which balances maximizing Q-values with a behavioral cloning regularization term to remain within the support of the offline data. During deployment, π_{low} serves as a local controller that reliably tracks the edges of the high-level plan.

4.4 Task-Specific Latent Graph Augmentation

The latent graph $\mathcal{H}_{\text{graph}}$ constructed in Section 4.2 encodes the purely geometric reachability structure of the environment. However, LTL specifications are defined over symbolic predicates (atomic propositions) in the task space. To bridge this *semantic gap* between the continuous latent manifold and the discrete logical constraints, we must augment the graph with task-specific semantic information.

Since the latent nodes originate from unsupervised clustering, they are spatially abstract and do not explicitly encode whether they reside within task-relevant regions (e.g., obstacles or goal zones). To resolve this ambiguity, we introduce two complementary annotation mechanisms: (i) *Soft Labels*, which provide a probabilistic estimate of region occupancy for conservative safety checking, and (ii) *Anchor Nodes*, which serve as certified waypoints for verifying proposition satisfaction.

Soft Label Estimation via Cluster Statistics. Each node $v \in \mathcal{V}$ in the latent graph represents a cluster of raw states, denoted as $\text{node2raw}(v)$, which were grouped together during the TD-aware clustering process. Because the embedding function ψ is non-invertible, we cannot analytically decode a latent coordinate back to the state space to check its label. Instead, we exploit the preserved set $\text{node2raw}(v)$ to perform statistical inference.

Let $\mathcal{AP} = \{\ell_1, \dots, \ell_m\}$ be the set of atomic propositions, where each ℓ_k corresponds to a labeled region $\mathcal{R}_{\ell_k} \subseteq \mathcal{X}$ in the task space. Using the projection map $\Pi : \mathcal{S} \rightarrow \mathcal{X}$, we quantify the degree of association between a latent node v and a label ℓ_k as the empirical probability that a state belonging to cluster v lies within \mathcal{R}_{ℓ_k} :

$$P(\ell_k \mid v) = \frac{|\{s \in \text{node2raw}(v) \mid \Pi(s) \in \mathcal{R}_{\ell_k}\}|}{|\text{node2raw}(v)|}. \quad (4)$$

Optionally, this estimation can be refined by weighting the contribution of each raw state based on its proximity to the cluster centroid in the latent space. This value $P(\ell_k \mid v) \in [0, 1]$ serves as a *soft semantic label*. It captures the heterogeneity of the cluster: a value close to 1 indicates that the node is almost entirely contained within the labeled region, whereas a value close to 0 implies it is disjoint. In our planning framework (Section 4.5), these soft labels are employed to determine the *feasibility* of transitions regarding negated constraints. Specifically, we introduce a safety threshold τ_{soft} . Any node v with $P(\ell_k \mid v) \geq \tau_{\text{soft}}$ is considered “unsafe” with respect to ℓ_k and is strictly excluded from transitions that forbid this label.

Anchor Node Insertion for Certified Liveness. While soft labels effectively characterize existing nodes, they are insufficient for guaranteeing the *satisfaction* of logical goals. A cluster might partially overlap with a target region \mathcal{R}_{ℓ} , but reaching the cluster center does not guarantee the agent physically enters \mathcal{R}_{ℓ} . To address this, we explicitly inject “certified” states into the graph.

For each atomic proposition $\ell_k \in \mathcal{AP}$ associated with region \mathcal{R}_{ℓ_k} , we require a set of representative raw states $\{s_j^{(\ell_k)}\}_{j=1}^{N_s} \subset \mathcal{S}$ whose projections satisfy $\Pi(s_j^{(\ell_k)}) \in \mathcal{R}_{\ell_k}$. These states are obtained via one of two methods depending on the problem domain:

- **State Construction:** If the mapping from task space to state space is partially invertible (e.g., specifying a position and appending zero velocities), we sample coordinates uniformly from \mathcal{R}_{ℓ_k} and *construct* the corresponding full states.
- **Dataset Retrieval:** Alternatively, if state construction is non-trivial, we *retrieve* states from the offline dataset \mathcal{D} that are verified to lie within \mathcal{R}_{ℓ_k} .

The obtained raw states are then embedded into the latent space to form new *anchor nodes*:

$$v_j^{(\ell_k)} = \psi(s_j^{(\ell_k)}), \quad \forall j \in \{1, \dots, N_s\}.$$

These new nodes are added to the vertex set: $\mathcal{V} \leftarrow \mathcal{V} \cup \{v_j^{(\ell_k)}\}$. Unlike standard nodes, anchor nodes are assigned deterministic semantic properties:

$$\text{is_anchor}(v_j^{(\ell_k)}) = \text{True}, \quad \text{anchor_label}(v_j^{(\ell_k)}) = \ell_k.$$

Connectivity Update. We integrate these anchor nodes into the graph structure by establishing edges according to the same temporal-distance criterion described in Section 4.2. To guarantee graph connectivity, in the rare case where an anchor

node remains isolated (i.e., no existing nodes fall within the distance threshold H_{TD}), we explicitly force a connection between the anchor and its nearest neighbor in the latent space.

Summary. The augmented graph now contains two distinct layers of semantic information. *Anchor nodes* provide precise, certified targets required to satisfy positive literals in the LTL formula. Conversely, *soft labels* provide a risk metric for existing nodes, enabling the planner to strictly prune transitions that might violate negative literals. This dual representation allows for robust planning over the continuous latent space.

4.5 High-Level LTL Task Planning

We now describe how the augmented latent graph is utilized to synthesize behaviors that satisfy a given LTL task. The core strategy is to perform an automata-theoretic search over the *product* of the LTL specification and the latent graph. This approach rigorously enforces temporal logic constraints while leveraging the latent geometry to ensure physical feasibility and minimize execution duration.

Büchi Automaton Construction. Given an LTL formula ϕ over atomic propositions \mathcal{AP} , we first translate it into a Non-deterministic Büchi Automaton (NBA) $\mathcal{B} = (Q, Q_0, \Sigma, \delta, F)$ using standard tools such as `ltl2ba` Gastin and Oddoux (2001). This automaton encodes the high-level task structure. Before planning, we simplify \mathcal{B} by pruning transitions that require the simultaneous satisfaction of multiple distinct propositions, as the labeled regions \mathcal{R}_ℓ are assumed to be disjoint in the task space. Additionally, we remove any accepting states that are topologically unreachable from the initial set Q_0 . These preprocessing steps yield a compact automaton that accelerates the downstream search.

Weighted Product System. Planning proceeds over the implicit product system $\mathcal{P} = \mathcal{H}_{\text{graph}} \otimes \mathcal{B}$, where the state space is $\mathcal{V} \times Q$. Let (v, q) be the current product state and (v', q') be a potential successor. A transition $((v, q) \rightarrow (v', q'))$ is considered *feasible* if and only if it satisfies both geometric and semantic constraints:

- (1) **Latent Reachability:** The nodes must be connected in the latent graph, i.e., $(v, v') \in \mathcal{E}$.
- (2) **Label Consistency:** Let the automaton transition be defined by a propositional formula σ such that $q' \in \delta(q, \sigma)$. We assume σ requires at most one positive literal ℓ_{req} and forbids a set of literals $\mathcal{F}_{\text{forb}}$. The target node v' must satisfy:
 - **Positive Constraint:** If ℓ_{req} exists, v' must be an **anchor node** with $\text{anchor_label}(v') = \ell_{\text{req}}$.
 - **Negative Constraint:** For all forbidden labels $\ell \in \mathcal{F}_{\text{forb}}$, v' must be “safe” with respect to the soft label estimate, i.e., $P(\ell \mid v') < \tau_{\text{soft}}$. Additionally, if v' is an anchor, its label must not be in $\mathcal{F}_{\text{forb}}$.

Crucially, this mechanism ensures that *anchor nodes* are used to certify progress (satisfying positive literals), while *soft labels* act as conservative filters to prevent violations of safety constraints. The cost of a feasible transition is inherited purely from the latent geometry: $c((v, q) \rightarrow (v', q')) = w(v, v') = \|v - v'\|_2$. We construct this product graph on-the-fly to avoid state explosion.

Prefix-Suffix Synthesis. To generate a satisfying infinite trajectory, we seek a plan consisting of a finite *prefix* Γ_{pre} reaching an accepting state, and a *suffix* cycle Γ_{suf} that visits the accepting set infinitely often.

1) **Prefix Search:** Let (v_0, q_0) be the initial product state, where $v_0 = \arg \min_{v \in \mathcal{V}} \|\psi(s_0) - v\|_2$ and q_0 is the initial automaton state. We employ A* search to find a path to an accepting product state (u, q^*) where $q^* \in F$. The heuristic function $h(v, q)$ is defined as the shortest latent distance to the nearest anchor node that satisfies a positive literal enabling a transition out of q . This heuristic is admissible and guides the search toward semantically relevant regions. Rather than terminating at the first solution, we retain the top- K cost-minimal *prefix paths* as candidates for the subsequent cycle construction phase.

2) **Suffix Cycle Construction:** For each candidate prefix endpoint (u, q^*) , we aim to construct a cycle returning to (u, q^*) . First, we check for a trivial solution: if the self-transition $(u, q^*) \rightarrow (u, q^*)$ is *feasible* in the product system (i.e., u satisfies any positive label requirements of the automaton self-loop $q^* \rightarrow q^*$ and respects all negative constraints), it constitutes a valid suffix cycle with zero cost. Otherwise, we search for a return path in the product space: $(u, q^*) \rightsquigarrow (u', q^*)$. Note that while the automaton state returns to q^* , the physical latent node may end at a different location u' . To close the physical loop, we compute a shortest path $u' \rightsquigarrow u$ purely within the latent graph, ensuring that all intermediate nodes remain safe with respect to any constraints imposed by the automaton state q^* .

3) **Optimization Objective:** Among all valid prefix-suffix pairs found, we select the optimal plan $\Gamma^* = \Gamma_{\text{pre}} \oplus \Gamma_{\text{suf}}^\omega$ that minimizes the weighted total length:

$$J(\Gamma) = \lambda \cdot \text{Cost}(\Gamma_{\text{pre}}) + (1 - \lambda) \cdot \text{Cost}(\Gamma_{\text{suf}}), \quad (5)$$

where $\text{Cost}(\cdot)$ sums the latent edge weights. The parameter $\lambda \in [0, 1]$ allows the user to trade off between the efficiency of the initial task completion and the compactness of the recurring behavior.

Remark 2. Recall that the latent space is trained such that Euclidean distances approximate the minimal temporal delay (steps-to-go) between states. Consequently, optimizing the geometric objective $J(\Gamma)$ acts as a direct proxy for minimizing the actual physical execution time $J(\tau)$. By tracking this high-level plan with a temporally-consistent low-level policy, the system realizes behaviors that are both logically correct and temporally efficient.

4.6 Low-Level Execution

Once the high-level plan $\Gamma = \Gamma_{\text{pre}} \oplus \Gamma_{\text{suf}}^\omega$ is synthesized, the agent executes it in the physical environment. The plan consists of a structured sequence of latent nodes $\Gamma = (v_0, v_1, \dots)$, where a subset of these nodes are *anchor nodes* certifying the satisfaction of atomic propositions. The objective of this stage is to control the dynamical system to traverse these latent waypoints sequentially, ensuring that all logical constraints are met and the Büchi acceptance condition is realized.

Sequential Waypoint Tracking. At each time step t , the agent embeds its current state s_t into the latent space as $h_t = \psi(s_t)$. To ensure robust execution without backtracking, we maintain a monotonically increasing *progress index* k pointing to the current target node v_k in the plan Γ . At each step, we search forward from the current index k to identify the furthest node $v_{k'}$ (where $k' \geq k$) that remains reachable within the temporal distance threshold (i.e., $\|h_t - v_{k'}\|_2 \leq H_{TD}$). We then update the target index to k' and set the local goal as $v_{k'}$. The low-level policy generates the action $a_t \sim \pi_{\text{low}}(s_t, \mathbf{h}_{\text{dir}})$ conditioned on the direction to this goal:

$$h_{\text{dir}} = \frac{v_{k'} - h_t}{\|v_{k'} - h_t\|_2}.$$

By strictly enforcing $k' \geq k$, this mechanism prevents the agent from reverting to previously tracked nodes (chattering), ensuring smooth and continuous progress along the planned trajectory while respecting the topological constraints of the graph.

Anchor Verification and Cycle Execution. Special handling is applied when the target node v_k is an *anchor node*. Unlike intermediate nodes which can be traversed loosely, anchor nodes represent semantic milestones. An anchor v_{anc} is declared *reached* only when:

$$\|\psi(s_t) - v_{\text{anc}}\|_2 < \varepsilon_{\text{anc}} \wedge L(s_t) = \text{anchor_label}(v_{\text{anc}}), \quad (6)$$

where ε_{anc} is a proximity threshold and $L(s_t)$ denotes the labels satisfied by the current state. Strictly enforcing this condition ensures that the physical system truthfully visits the semantic regions required by the LTL specification.

Upon reaching the final node of the prefix Γ_{pre} , the agent seamlessly transitions to the first node of the suffix Γ_{suf} . Similarly, when the last node of the suffix is reached, the tracking index resets to the beginning of Γ_{suf} . This cyclic execution continues indefinitely, satisfying the infinite visitation requirement of the Büchi automaton.

5. EXPERIMENTS

5.1 Experimental Setup

Environments and Datasets. We evaluate our framework on the `antmaze` domain of **OGBench** Park et al. (2025), a challenging benchmark designed for offline goal-conditioned RL. OGBench specifically targets difficulties such as long-horizon reasoning, hierarchical stitching, and robustness to heterogeneous data quality. In this environment, the agent controls an 8-DoF quadruped robot (29-dimensional state space) to navigate complex continuous mazes. We conduct experiments across three complexity scales: *medium*, *large*, and *giant*. The *giant* maze variants, in particular, impose significant challenges, requiring planning over extremely long horizons and reliable stitching of disparate trajectory fragments.

We utilize three distinct data-collection regimes provided by OGBench:

- `navigate`: Noisy expert demonstrations reaching random goal locations.
- `stitch`: Short, fragmented trajectories that do not connect start and goal states directly, necessitating multi-stage stitching.
- `explore`: Random exploratory rollouts with low-quality behavioral coverage.

Crucially, these datasets are *task-agnostic*: they contain only short-term motion primitives and do not demonstrate the complex temporal behaviors required by our LTL specifications. This setup strictly adheres to our problem formulation, where the agent must synthesize long-horizon solutions solely from fragmented offline data.

LTL Task Generation. To assess the logical reasoning capabilities of our method, we construct a benchmark of random LTL-X tasks. We define a set of *task templates* (see Table 1) capturing diverse temporal properties, including safety (avoidance), liveness (visitation), sequentiality, and recurrence. These templates

are parameterized by a variable number of atomic propositions. Complex specifications are generated by composing multiple templates via logical conjunction.

For each generated formula, we perform a validity check: we construct the corresponding Büchi automaton, prune infeasible transitions (e.g., mixed-positive requirements), and verify the graph-theoretic reachability of accepting states. Once a valid formula is obtained, we ground the atomic propositions into the environment by generating random geometric regions (e.g., circles, rectangles, or polygons). These regions are guaranteed to be located in free space and are pairwise disjoint to ensure semantic consistency.

Table 1. Examples of LTL Task Templates

LTL Formula Structure	Semantic Description
$F\ell_i$	Reach: Eventually visit region i .
$G(\neg\ell_i)$	Safety: Always avoid region i .
$F(\ell_1 \wedge F(\ell_2 \wedge \dots \wedge F\ell_m))$	Sequence: Visit $1 \rightarrow 2 \rightarrow \dots \rightarrow m$.
$F\ell_1 \wedge F\ell_2 \wedge \dots \wedge F\ell_m$	Coverage: Visit m regions (any order).
$\neg\ell_{\text{avoid}} \text{ U } \ell_{\text{goal}}$	Conditional: Avoid until goal is reached.
$GF(\ell_1 \wedge F(\ell_2 \wedge \dots \wedge F\ell_m))$	Patrol: Infinitely revisit $1 \rightarrow \dots \rightarrow m$.
$F(\ell_1 \vee \ell_2 \vee \dots \vee \ell_m)$	Choice: Visit at least one region in set.

Note: F (Eventually), G (Always), and U (Until) denote standard LTL operators. These templates represent a subset of patterns; the number of propositions (m) varies per task.

Evaluation Protocol. We adopt a unified evaluation protocol across all experiments. The offline phase, which comprises latent graph construction (Section 4.2) and low-level policy training (Section 4.3), is performed *once* per dataset, independent of downstream tasks. During the online phase, LTL specifications are introduced, and we execute the planning pipeline (Section 4.4–4.6). To evaluate success, we verify whether the executed trajectory satisfies the generated LTL formula. For tasks involving infinite recurrence (suffix cycles), we consider the task successful if the agent completes the prefix and successfully traverses the suffix cycle *once*, as this physically validates the feasibility of the recurring behavior.

5.2 Case Study

To qualitatively validate the capability of SAGAS in composing long-horizon behaviors from fragmented data, we examine a challenging scenario in the `antmaze-giant-stitch` environment. In this setting, both the robot dynamics and the maze layout are unknown. As detailed in Section 5.1, the offline dataset \mathcal{D} consists exclusively of short, task-agnostic trajectory fragments, with no single trajectory satisfying the target temporal pattern.

We evaluate SAGAS on a complex composite LTL specification:

$$\underbrace{G(F(e_1 \wedge F(e_2 \wedge F e_3)))}_{\text{Infinite Patrol}} \wedge \underbrace{F(e_4 \wedge F(e_5 \wedge F e_6))}_{\text{Sequential Visit}} \wedge \underbrace{(\neg e_5 \text{ U } e_7)}_{\text{Conditional Safety}}. \quad (7)$$

This specification imposes three concurrent objectives: (i) Infinitely repeat the patrol sequence $e_1 \rightarrow e_2 \rightarrow e_3$; (ii) Complete the visitation sequence $e_4 \rightarrow e_5 \rightarrow e_6$; (iii) Satisfy a safety constraint forbidding entry into e_5 until e_7 is visited. Note that the combination of (ii) and (iii) implicitly requires the agent to *detour* to e_7 before it can progress through e_5 .

The resulting execution trajectory is visualized in Fig. 2. Starting from the initial state (red dot), the agent realizes the prefix

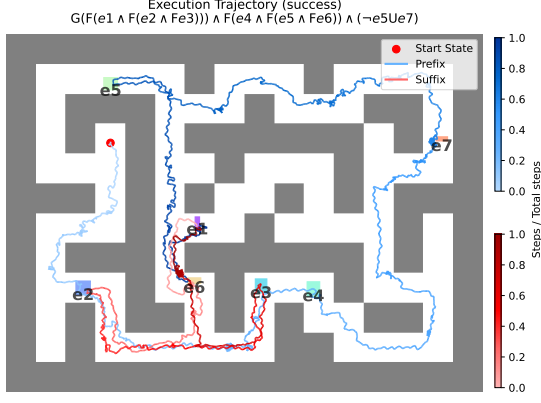


Fig. 2. Execution trajectory for the LTL task defined in Eq. (7).

phase (blue trajectory) before seamlessly transitioning into the recurring suffix loop (red trajectory). The trajectory shows that the agent successfully fulfills all concurrent objectives: it correctly prioritizes the detour to e_7 to satisfy the safety constraint before completing the sequence and converging to the limit cycle. This underscores the efficacy of SAGAS: by integrating latent-graph reasoning with automata-guided planning, SAGAS enables the reliable execution of highly structured, long-horizon LTL tasks where neither demonstrations nor dynamic models are available.

5.3 Large-Scale Experiments

Task Complexity Levels. We categorize randomly generated LTL tasks into three difficulty levels based on logical composition and the number of atomic propositions: (1) **Simple**: Simple templates without boolean composition, involving ≤ 5 labeled regions; (2) **Medium**: Composition of up to 3 templates, involving ≤ 5 regions; (3) **Hard**: Complex composition of up to 4 templates involving ≤ 8 regions. For each setting, we evaluate 200 unique tasks, each executed from 5 distinct initial states, totaling 1000 evaluation episodes.

Performance Metrics. We report: (1) **SR (%)**: Success Rate; (2) **Time (s)**: Planning Time; (3) **Len**: Average Trajectory Length.

Results and Analysis. Table 2 summarizes the results, highlighting three key strengths of SAGAS:

Robustness to Heterogeneous Data. Notably, SAGAS performs exceptionally well on *stitch* and *explore* datasets, often surpassing the expert-like navigate regime (e.g., 89.9% vs 80.9% in *AntMaze-Large*). This trend aligns with results in GAS Baek et al. (2025), as we adopt consistent TD learning and low-level policy parameters. It confirms that the latent graph effectively recovers global connectivity from suboptimal, fragmented data.

Scalability to Giant Maps. The framework scales effectively to *AntMaze-Giant*, handling horizons exceeding 2000 steps while maintaining 70% success rates for *Simple/Medium* tasks. Planning time remains negligible ($< 3s$), demonstrating that graph abstraction successfully compresses the state space, thereby preventing the combinatorial explosion typical of long-horizon LTL planning.

Execution Stability vs. Logical Complexity. Performance remains stable between *Simple* and *Medium* tasks (drop $< 4\%$). Even under the most demanding *Hard* setting (involving up to 8

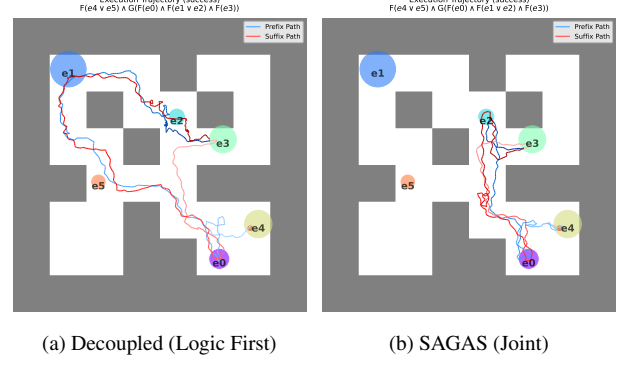


Fig. 3. Trajectory comparison on a Hard task: (a) Decoupled Baseline vs. (b) SAGAS (Ours).

regions and 4 templates), our framework retains substantial success rates (e.g., $> 54\%$ in *Giant-Stitch*), experiencing only a moderate decline despite the trajectory length nearly doubling. Failure analysis reveals that this drop is primarily due to mechanical instability (e.g., agent flipping) during such extended execution, rather than planning failures. This confirms that our high-level planner remains robust, correctly synthesizing logic-satisfying plans even when physical execution becomes the limiting factor.

Ablation: Joint Product Search vs. Decoupled Planning. To validate our method’s ability to minimize the execution cost $J(\tau)$, we compared SAGAS against a **Decoupled Planning** baseline. This baseline adopts a **prioritized optimization** strategy: it first identifies a sequence of transitions that minimizes *logical hops* on the Büchi automaton, and subsequently uses GAS to plan the shortest latent path for each specific transition. While this ensures logical correctness, it decouples the decision-making process, often selecting logically adjacent but geometrically distant subgoals (as visualized in Fig. 3). In contrast, SAGAS performs **joint optimization** directly in the product space, allowing the planner to trade off logical steps for physical efficiency. Quantitative results on 100 additional *Hard* cases confirm this advantage: SAGAS achieves a higher success rate ($91.0 \pm 9.2\%$ vs. $83.0 \pm 6.0\%$) and reduces the average trajectory length (618.7 ± 326.1 vs. 705.0 ± 395.2) by $\approx 12\%$. This proves that our **semantic-aware graph** enables true joint planning, synthesizing behaviors that are physically efficient rather than just logically minimal.

6. CONCLUSION

In this work, we presented **SAGAS**, a hierarchical framework for planning arbitrary Linear Temporal Logic (LTL) specifications in a fully offline, model-free setting. By bridging graph-assisted trajectory stitching with automata-theoretic approach, our framework effectively recovers long-horizon connectivity from fragmented, task-agnostic datasets. We introduced a semantic augmentation mechanism to ground logical propositions in a learned latent space and developed a cost-aware product search algorithm to synthesize efficient prefix-suffix plans. Experiments on the OGBench benchmark demonstrate that our method scales robustly to giant-scale environments and heterogeneous data qualities, significantly outperforming baselines that lack global structural reasoning. Future work will extend this paradigm to high-dimensional visual observations and explore probabilistic guarantees for safety-critical applications in dynamic environments.

Table 2. Quantitative Results on Large-Scale LTL Tasks

Map Size	Dataset	Simple Tasks			Medium Tasks			Hard Tasks		
		SR (%)	Time (s)	Len	SR (%)	Time (s)	Len	SR (%)	Time (s)	Len
Medium	navigate	80.1 ± 21.5	1.32 ± 1.60	795.5 ± 433.3	77.4 ± 21.7	1.12 ± 1.19	831.1 ± 496.4	58.2 ± 34.6	3.97 ± 7.07	1211.5 ± 772.6
	stitch	83.6 ± 20.8	2.25 ± 2.74	865.3 ± 558.9	81.9 ± 23.6	1.87 ± 2.03	821.1 ± 528.9	65.9 ± 34.6	7.81 ± 13.92	1264.7 ± 787.7
	explore	90.1 ± 23.8	2.32 ± 3.05	548.9 ± 400.4	88.1 ± 25.4	1.90 ± 2.05	526.0 ± 387.3	76.5 ± 37.6	7.42 ± 13.93	895.7 ± 1020.1
Large	navigate	80.9 ± 23.4	1.28 ± 1.57	1177.5 ± 673.0	77.5 ± 25.1	1.11 ± 1.17	1167.8 ± 579.0	56.9 ± 34.5	3.47 ± 5.48	1767.0 ± 1185.7
	stitch	82.7 ± 20.8	2.72 ± 3.45	1205.3 ± 683.7	79.7 ± 24.1	2.34 ± 2.52	1271.5 ± 703.3	60.8 ± 35.1	8.66 ± 14.73	1778.0 ± 1044.0
	explore	89.9 ± 21.2	3.20 ± 4.19	793.6 ± 467.9	89.2 ± 22.0	2.79 ± 3.16	904.9 ± 546.3	70.5 ± 37.0	10.16 ± 16.30	1335.8 ± 900.9
Giant	navigate	69.7 ± 23.8	0.75 ± 0.94	1590.9 ± 807.9	71.5 ± 23.1	0.64 ± 0.70	1557.5 ± 752.5	49.9 ± 31.6	2.16 ± 3.47	2282.5 ± 1333.1
	stitch	72.3 ± 23.0	2.89 ± 3.67	2050.9 ± 942.8	68.8 ± 25.5	2.43 ± 2.72	2092.9 ± 929.4	54.3 ± 31.6	8.85 ± 14.43	2905.6 ± 1639.9

Note: Results are presented as Mean ± Standard Deviation. **SR**: Success Rate; **Time**: Planning wall-clock time; **Len**: Average total trajectory length (prefix + suffix).

DECLARATION OF GENERATIVE AI AND AI-ASSISTED TECHNOLOGIES IN THE WRITING PROCESS

During the preparation of this work the author(s) used ChatGPT in order to improve the readability and language. After using this tool/service, the author(s) reviewed and edited the content as needed and take(s) full responsibility for the content of the publication.

REFERENCES

- Andrychowicz, M., Wolski, F., Ray, A., Schneider, J., Fong, R., Welinder, P., McGrew, B., Tobin, J., Pieter Abbeel, O., and Zaremba, W. (2017). Hindsight experience replay. *Advances in neural information processing systems*, 30.
- Baek, S., Park, T., Park, J., Oh, S., and Kim, Y. (2025). Graph-assisted stitching for offline hierarchical reinforcement learning. *arXiv preprint arXiv:2506.07744*.
- Bagatella, M., Krause, A., and Martius, G. (2024). Directed exploration in reinforcement learning from linear temporal logic. *Transactions on Machine Learning Research*.
- Baier, C. and Katoen, J.P. (2008). *Principles of model checking*. MIT press.
- Fainekos, G.E., Kress-Gazit, H., and Pappas, G.J. (2005). Temporal logic motion planning for mobile robots. In *Proceedings of the 2005 IEEE International Conference on Robotics and Automation*, 2020–2025. IEEE.
- Feng, Z., Luan, H., Ma, K.Y., and Soh, H. (2025). Diffusion meets options: Hierarchical generative skill composition for temporally-extended tasks. In *2025 IEEE International Conference on Robotics and Automation (ICRA)*, 10854–10860. IEEE.
- Fujimoto, S. and Gu, S.S. (2021). A minimalist approach to offline reinforcement learning. *Advances in neural information processing systems*, 34, 20132–20145.
- Gastin, P. and Oddoux, D. (2001). Fast ltl to büchi automata translation. In *International Conference on Computer Aided Verification*, 53–65. Springer.
- Guo, Z., Işık, İ., Ahmad, H., and Li, W. (2025). One subgoal at a time: Zero-shot generalization to arbitrary linear temporal logic requirements in multi-task reinforcement learning. *arXiv preprint arXiv:2508.01561*.
- Hasanbeig, M., Abate, A., and Kroening, D. (2018). Logically-constrained reinforcement learning. *arXiv preprint arXiv:1801.08099*.
- Jackermeier, M. and Abate, A. (2025). Deepltl: Learning to efficiently satisfy complex ltl specifications for multi-task rl. In *The Thirteenth International Conference on Learning Representations*.
- Kloetzer, M. and Belta, C. (2008). A fully automated framework for control of linear systems from temporal logic specifications. *IEEE Transactions on Automatic Control*, 53(1), 287–297.
- Kostrikov, I., Nair, A., and Levine, S. (2022). Offline reinforcement learning with implicit q-learning. In *International Conference on Learning Representations*.
- Liu, J.X., Shah, A., Rosen, E., Jia, M., Konidaris, G., and Tellex, S. (2024). Skill transfer for temporal task specification. In *2024 IEEE International Conference on Robotics and Automation (ICRA)*, 2535–2541. IEEE.
- Opryshko, E., Quan, J., Voelcker, C., Du, Y., and Gilitschenski, I. (2025). Test-time graph search for goal-conditioned reinforcement learning. *arXiv preprint arXiv:2510.07257*.
- Park, S., Frans, K., Eysenbach, B., and Levine, S. (2025). OGBench: Benchmarking offline goal-conditioned RL. In *The Thirteenth International Conference on Learning Representations (ICLR)*.
- Park, S., Ghosh, D., Eysenbach, B., and Levine, S. (2023). Hlq: Offline goal-conditioned rl with latent states as actions. *Advances in Neural Information Processing Systems*, 36, 34866–34891.
- Qiu, W., Mao, W., and Zhu, H. (2023). Instructing goal-conditioned reinforcement learning agents with temporal logic objectives. *Advances in Neural Information Processing Systems*, 36, 39147–39175.
- Ren, J., Miller, H., Feigh, K.M., Coogan, S., and Zhao, Y. (2024). Ltl-d*: Incrementally optimal replanning for feasible and infeasible tasks in linear temporal logic specifications. In *2024 IEEE/RSJ International Conference on Intelligent Robots and Systems (IROS)*, 4495–4502. IEEE.
- Scher, G. and Kress-Gazit, H. (2020). Warehouse automation in a day: from model to implementation with provable guarantees. In *IEEE International Conference on Automation Science and Engineering*, 280–287.
- Shah, A., Voloshin, C., Yang, C., Verma, A., Chaudhuri, S., and Seshia, S.A. (2024). Ltl-constrained policy optimization with cycle experience replay. *Transactions on Machine Learning Research*.
- Smith, S.L., Tümová, J., Belta, C., and Rus, D. (2011). Optimal path planning for surveillance with temporal-logic constraints. *The International Journal of Robotics Research*, 30(14), 1695–1708.
- Vasile, C.I. and Belta, C. (2013). Sampling-based temporal logic path planning. In *International Conference on Intelligent Robots and Systems*, 4817–4822.
- Voloshin, C., Verma, A., and Yue, Y. (2023). Eventual discounting temporal logic counterfactual experience replay. In *International Conference on Machine Learning*, 35137–35150. PMLR.